Proceedings of ASME Turbo Expo 2020
Turbomachinery Technical Conference and Exposition
GT2020
September 21-25, 2020, Virtual, Online

GT2020-14631

COMPRESSED AIR ENERGY STORAGE FOR A SMALL SIZE STANDALONE PLANT POWERED BY A SOLAR POWER UNIT AND A GAS TURBINE

Gianmario L. Arnulfi, Giulio Croce

University of Udine
Polytechnic Department of Engineering and Architecture
Udine, Italy

ABSTRACT

Energy storage can balance heat and power demand and production over different time scales, with both technical and economic benefit. Several devices have been proposed, but only two are really utilized: hydro-pumped storage, for large size plants, and electrochemical battery energy storage, for medium and small plants. Compressed Air Energy Storage (CAES) was proposed as an alternative, and two well-known plants, Hunthorf (Germany) and Mac Intosh (United States) have been successfully working for many years. However, due to the huge capital costs, this concept never became widely popular. Here, a bit different approach is proposed: one or more reciprocating compressors and pressurized reservoirs can supply an additional amount of air to a gas turbine. During the "charging" phase, the reciprocating compressors pump air into the reservoirs; during the "discharging" phase, the turbo-expander is fed by both the turbo-compressor and the reservoirs in parallel. The turbo-compressor is partially relieved and fuel can be saved for the same power. This paper focuses on a standalone small size user, served by a solar power unit coupled with a micro gas turbine. The aim is to lay down rules for a proper storage managing.

Keywords: Energy storage; Gas turbine; CAES.

NOMENCLATURE

D	discharge degree
E	energy
H	relative apparent efficiency
L	charge level
m	mass
$\dot{m}$	mass flow rate
P	power
p	pressure
R	*ratio*
Q	fuel heat
t	time
W	work

Subscript	
d	design point
AD	air discharging
AS	air storage
SC	storage compressor
s	solar
US	solar output minus user load
U	user
0	inlet total condition
Superscripts	
X	ratio vs. GT design point.
Acronyms	
BS	battery storage
CAES	compressed air energy storage
GT	gas turbine
PG	power grid
TESTIAC	thermal energy storage (gas) turbine air-cooling
TS	thermal storage

1. INTRODUCTION

Widespread concern for the current climate change led, in the past decade, to an exponential increase in renewable energy production. Stochastic energy sources, such as wind and sun, play a major role, since the contribution from the large scale reservoir hydro power in most industrialized countries is close to saturation. The lack of control on the primary energy supply poses a challenge on the grid management, fostering a growing interest in storage systems. In particular, there is a significant shift in the drivers for grid-related energy storage: in the past, the interest was in large systems designed to take advantage from the price differential between peak and night hours; now, the main motivation is related to the management of the mismatch

between the timing of renewable energy production and the timing of end user consumption.

As an example, in Italy, even if the yearly share of photovoltaic energy is still low, it is quite possible to have overproduction in a clear summer day or locally exceed the grid transmission capacity. Furthermore, the challenges involved in the management of a large grid fed by a huge number of small, stochastic plants has already motivated several utilities to promote the use of small scale local storage for domestic scale solar systems. Thus, in several cases there is a strong need for a small to medium size storage.

The two most mature technologies for energy storage are by far the hydro-pumped and electrochemical systems: the former are best suited to large scale plant, the latter for small or at most medium sized application. However, open literature offers a wide range of alternative approaches, from chemical storage (power to fuel) to compressed air systems (CAES) and even mechanical devices (flywheels).

In the original CAES systems [1], initially proposed for large scale application, electric power is produced via a Brayton-Joule cycle, but the compression and expansion processes are decoupled physically and in time. An electrically driven compressor fills a high pressure storage, while the combustion chamber and turbine are fed by the compressed air extracted from the storage. The system is, thus, a hybrid storage and production plant, since the discharge step requires fuel energy input in the combustion chamber. However, un-fired, purely storage systems have also been proposed [2], along with several combinations with thermal energy storage [1]. For large scale plants, the need for huge storage volumes involves significant site constraints: often natural caverns and/or exhausted natural gas fields are considered as feasible options.

Storage is much easier for the micro and mini configurations, removing siting constraints and making easier the coupling with local renewable energy sources. Thus, while large CAES systems has proven unpractical, the smaller size ones are often considered in literature, even for residential application [3]. This is due to the relatively low cost of the equipment: a small pressure tank and a compressor, usually a reciprocating one. Micro gas turbines generally have a low pressure ratio, thus allowing for cheaper storage equipment, may in principle require less maintenance with respect to other backup generation systems, and their compact size leaves room for the storage equipment.

Thus, a number of plants have been proposed in open literature: to name a few examples, in [4] a medium scale system, with a 500 kW input power and an 8 hour discharge design time is proposed as a tool to deal with renewable energy stochastic output; Villella et al. [5] support a stand-alone photovoltaic field with a small scale CAES; Jannelli et al. [6] present a micro unfired CAES plant, with compressor and turbine of the order of 1 kW, coupled with a 33 kW photovoltaic field, designed to provide energy to a mobile radio station; Zhang [7] considers an islanded microgrid fed by wind and solar energy, coupled with an unfired CAES.

A different plant, possibly less capital intensive, is proposed in [8, 9]: a standard GT turbine is considered, rather than separated compression and expansion machines, and the high pressure air from the storage is injected in the GT compressor outlet air stream ahead of the combustion chamber. Thus, for a given turbine mass flow and power output, the compressor elaborates a lower mass flow and requires less power, leading to an increase in the net power output from the gas turbine system. However, for any given rotation speed, the compressor must elaborate at least a defined minimum mass flow, to avoid stall and surge, thus defining the maximum possible storage discharge mass flow.

Here, we focus on a micro size plant. Namely, we consider a stand-alone, small scale application of the order of 100 kW of average power request, to be satisfied mainly via photovoltaic solar energy. A storage system is obviously required, but due to the significant cost of a medium to large electrochemical one, it is worth to investigate some cheaper alternative.

In particular, given the obvious need for a fossil fuel backup generator, to ensure the energy supply even in the worst case scenario, we consider a small scale auxiliary compressed air storage as in [9]. In such configuration, as described above, an off-the shelf commercial gas turbine is used: the compressed air from the storage allows for a reduction of the mass flow (and power requirement) through the GT plant compressor.

A lumped parameter model is used to predict the time evolution of the power plant, including a detailed prediction of the actual operating point of the GT system, taking into account the rotating speed variation and the impact of the storage mass flow contribution on the turbine/compressor matching.

Global energy performances are compared for two different load profile. We focus on a simple scheme, to investigate specifically the CAES performance in terms of saved primary energy and storage efficiency: any further development, including the presence of auxiliary electrochemical batteries or thermal storage additions will be considered in the future.

2. PLANT CONFIGURATION

The proposed plant is described in Fig. 1. An electric user (M) is served by a power station, which relies on two different primary sources: solar energy, via a photovoltaic system, and natural gas, via a micro gas turbine. The latter is necessary, to ensure a reliable energy supply regardless of available irradiance. A CAES storage system, including a positive displacement compressor, a compressed air tank and two cooling heat exchanger deals with the possible mismatch between solar energy supply and user requirement.

Note that all the valves are represented as a double triangle, as usual; double empty triangle denotes a proportional valve, double solid triangle an on/off valve and solid and empty triangle the check (non-return) valves, with the latter denoting the allowed way. In Fig. 1 a full-featured plant is considered, including some additional components that may be of future interest, but have not been modelled yet. These elements are reported in pink color and will not be considered in the present first step of this research. For instance, at present a stand-alone plant is assumed, so that electricity price is not relevant, and only

one energy storage device is provided. However, in the near future, the authors plan to add a power grid connection, maybe with a bottle-neck, an electrochemical battery storage and a thermal energy storage for gas turbine inlet air cooling (TESTIAC), similar to that already considered in Arnulfi et al. [10].

The gas turbine is similar to the Turbec T100, follows a heat exchange cycle, is fuelled by natural gas and its speed can be controlled by an inverter. Its rated data are shown in Table 1.

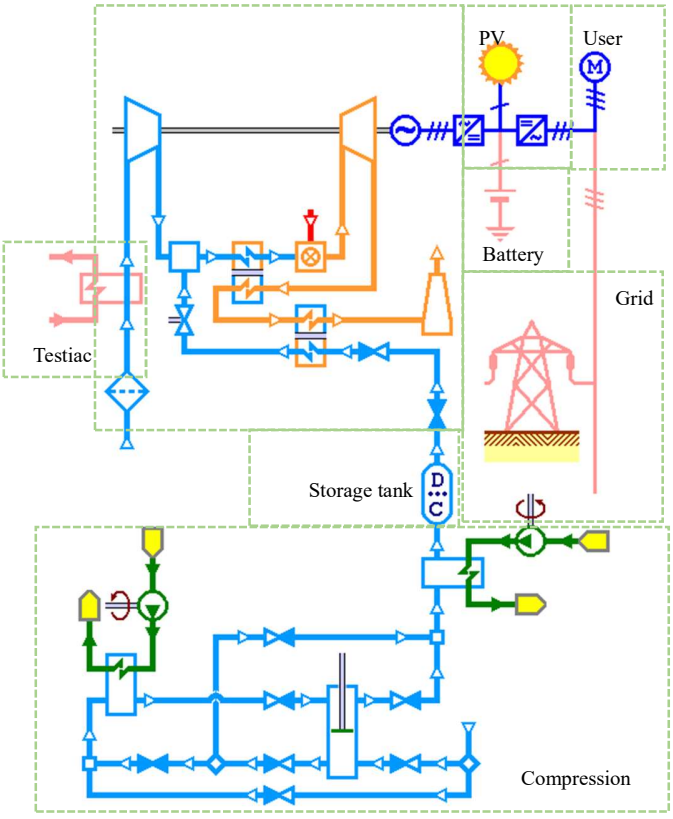

FIGURE 1: PLANT SCHEME.

The energy storage device includes six parallel connected units composed by a reservoir and a compressor. The former may be easily manufactured by using commercial methane pipeline. The latter is based on a double acting, reciprocating compressor, with rated data in Table 2. The two acting modes can work in both series and parallel. The processed air is inter- and after-cooled by means of two air-water heat exchangers. Cooling water is available at ambient temperature. The maximum available pressure is 5 MPa: such relatively low value is chosen to avoid the need for a third compression stage and for a more expensive, higher pressure tank.

The operational mode of the energy system can be described by Fig. 2. The arrow points denote the energy flow direction. At any time, either the operator or an optimizing algorithm decides if the energy storage device (AS) must charge, discharge or do nothing (green arrows). Looking at the sun-load surplus or deficit (gray arrows) it is thus possible to compute the required gas turbine power output and the corresponding fuel energy consumption (red arrows), always imposing that the algebraic sum of GT power output (positive), charge power (negative), sun electric output (positive) and load (negative) is zero. In Fig. 2, and in the following discussions, we indicate with US the sun load surplus, i.e. the difference between the solar output and the end user load, since this is the actual boundary condition CAES has to cope with.

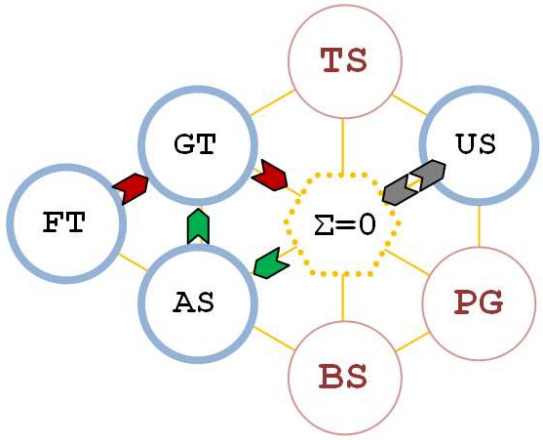

FIGURE 2: ENERGY STATION MAP. AS: air storage; GT: gas turbine; US: User load minus solar contribution; FT: fuel tank; TS: thermal storage (not included); PG: power grid (not included); BS: electrochemical battery (not included)

TABLE 1 GAS TURBINE RATED DATA

Pressure ratio	4.5	-
Turbine inlet temperature	1223	K
Exhaust gas mass flow rate	0.8	kg/s
Heat exchanger effectiveness	0.80	-
Power	100	kW
Efficiency	0.29	-

TABLE 2 STORAGE DEVICE RATED DATA

Number of units	6	
Reservoir volume	10	m^3
Piston bore	117	mm
Piston rod diameter	98	mm
Stroke	187	mm
Clearance volume	5%	
Speed	10	rps
Polytropic efficiency	0.9	

TABLE 3 ATMOSPHERIC CONDITIONS.

Pressure	100	kPa
Temperature	288	K
Humidity	45	%

TABLE 4 NON DIMENSIONALIZATION REFERENCES

$p_{cc,d}$	Combustion chamber pressure	450	kPa
$P_{GT,d}$	Net nominal GT power output	100	kW
$\dot{m}_{a,d}$	GT air mass flow rate	0.79	kg/s
t_{ref}	Processed cycle	24	hours
E_{ref}	Daily user energy requirement	2400	kWh

3. MATHEMATICAL MODELS

In general, the authors tried to use non-dimensional variables and parameters as far as possible. Any non-dimensional parameter, denoted by the x prime at left, is the ratio between a variable and its rated GT homologous, as in Table 4; thus, for power P, time t and energy E we define:

$$ {}^{x}P = \frac{P}{P_{GT,d}} \qquad {}^{x}t = \frac{t}{t_{ref}} \qquad {}^{x}E = \frac{E}{E_{ref}} \tag{1}$$

A lumped parameter, quasi-steady approach is adopted. For each single component, mass and energy balances are written and solved both in design and off-design conditions. The resulting set of ordinary differential equations driving the evolution of the storage charge state, energy consumption (fuel, charging and discharging air energy) and energy production (sun power and gas turbine shaft power) are solved by means of an explicit Euler algorithm. For the algebraic equations, the Newton-Raphson algorithm is utilized.

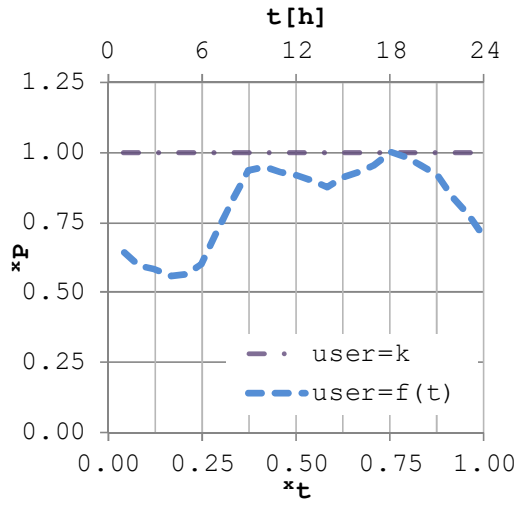

FIGURE 3: LOAD TIME SERIES

The analysis is carried out for a single representative day: two case studies, constant and variable load, are analyzed. Small scale grids can have quite different loads, ranging a from purely residential demand to highly variable profiles, strongly dependent on the characteristic of a single large industrial user. Thus, it is difficult to define a general profile: here, we scale down the global electric energy requirement on a sample day in the Italian national market, roughly representative of a mix of residential and industrial users.

Fig. 3 shows the two normalized load profiles along the day. Note that in both cases the load peak is assumed equal to the GT rated power. In the variable case the ratio between minimum and maximum load is quite low, at 0.56, and the maximum power requests occurs at daylight time, i.e. when the solar production is at its maximum.

The tanks are assumed iso-thermal; the reciprocating compressors are modelized, simply, by thermo-dynamic working cycle evaluation assuming a polytropic efficiency, as usual for positive displacement compressors, as suggested by Rogers and Mayhew [11]. Polytropic efficiency takes into account irreversibility, thermodynamic cycle shape, and mixing effects between the incoming air and air already present in the clearance volume. Polytropic ideal process is preferred vs. isentropic or isothermal essentially because it allows an estimation of real mass flow rate. Inter-stage pressure is found iteratively to ensure continuity in the inter-cooler volume.

The gas turbine is simulated following the matching procedure for the turbomachinery proposed by Cohen et al. [12]. For turbo-compressor and turbo-expander, power is calculated assuming a polytropic efficiency, function of blade Mach number and pressure ratio. Since starting and shutdown transients are not considered, the compressor always works in the stable range and the expander is supposed choked.

If we define the non-dimensional pressure and mass flow as:

$$ {}^{x}m = \frac{\dot{m}\sqrt{T_0}\ p_{0,d}}{\dot{m}_d\sqrt{T_{0,d}}\ p_0} \tag{2}$$

$$ {}^{x}p = \frac{R_p - 1}{R_{p,d} - 1} \tag{3}$$

the compressor map (Fig. 4) consists of a mesh of several lines at constant blade Mach number (i.e. equivalent rotating speed) and beta lines, as suggested by Kurzke [13]. The former, which have a clear and well-known physical meaning, are assumed as hyper ellipses (Arnulfi et al. [14]), the latter, which are mere convenient computational tools, are assumed as parabolas. Their only requirement is to be quasi-orthogonal to the iso-Mach but, as a single stage compressor is concerned, parabolas are also loci of working conditions at the same incidence angle (Pampreen [15]). Thus, as unsteady flow (rotating stall or surge) may appear when incidence angle grows up too much, a parabola may well represent the surge limit: the significance of this aspect will be explained in the following. The compressor map refers to atmospheric condition, here assumed as in Table 3.

Discharge degree and storage level are real numbers between 0.0 and 1.0, defined by Eq. (4) and (5) respectively, with maximum and minimum values defined in the following.

$$D = \frac{\dot{m}_{AD}}{\dot{m}_{AD}^{max}} \tag{4}$$

$$L = \frac{m_{AS} - m_{AS}^{min}}{m_{AS}^{max} - m_{AS}^{min}} \tag{5}$$

The maximum discharge mass flow $\dot{m}_{AD}^{max}$ is limited by compressor stability. In fact, we can define a GT operating point in terms of compressor required exit pressure, combustion chamber inlet air flow and compressor rotating speed. For any pressure ratio, on the other hand, the compressor mass flow rate cannot fall below the stall limit (i.e. the light blue line, defining the left limit of the compressor map in Fig. 4). Thus, for any given compressor pressure ratio, the maximum discharge flow $\dot{m}_{AD}^{max}$ is the difference between the combustion chamber inlet air flow and the compressor stall mass flow.

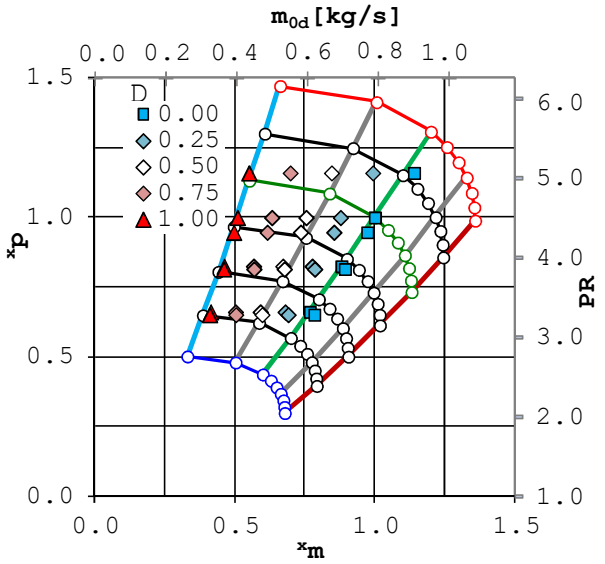

FIGURE 4: GT COMPRESSOR WORKING CONDITIONS.

The minimum and maximum mass in the storage $m_{AS}^{min}, m_{AS}^{max}$ are computed as the storage content at ambient temperature and minimum and maximum allowed pressure, respectively. The information in Fig. 4 are used to define the GT performance as a function of the discharge ratio D. In case of zero discharge, any operating point in Fig. 4 corresponds to a single possible operating point of the GT, and thus a single value of net power output. For any given power output, however, it is possible to look for the rotating speed that provides the maximum efficiency. The locus of such maximum efficiency points is indicated by the blue squares in Fig. 4. When the discharge is activated we chose to preserve the optimal inlet pressure and mass flow in the combustion chamber: thus, the operating point of the turbo expander and of the combustion chamber is not significantly affected, while the compressor operating point moves horizontally to the left in Fig. 4. Care must be taken to avoid overstep the surge limit, marked with red triangles in Fig 4. Diamonds denote different allowed working conditions during storage discharge.

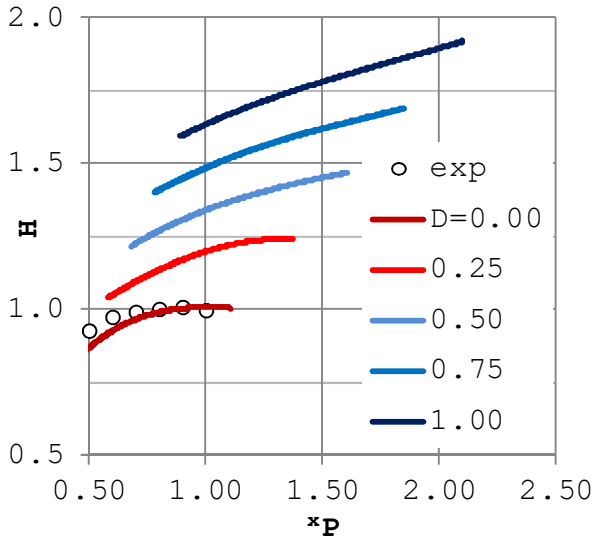

FIGURE 5: DISCHARGE PERFORMANCE AT DIFFERENT DISCHARGE DEGREES D.

Since the turbo expander output and combustion performances are roughly independent on D, while the GT compressor power reduces with D, the global effect is an increase in net GT power output with the same fuel consumption. This is shown in Fig. 5, where we plot, for different D, the increase in relative apparent efficiency

$$H = \left(\frac{P_{GT}}{\dot{m}_c}\right)\left(\frac{\dot{m}_{c,d}}{P_{GT,d}}\right) \tag{6}$$

It is evident that the net power supplied to the user is larger than the nominal GT power. At maximum storage discharge degree D, maximum power output is twice the nominal one: it is, thus, possible to use the discharge as a peak-shaving measure, allowing for a GT with a lower nominal power. Thus, the proposed storage device can save operational costs, due to fuel savings, but has also a complex effect on capital cost. Namely, we have an increase in capital cost due to the reciprocating compressors and storage equipment, but we may have also a reduction in the GT cost, if the discharge is used to satisfy the peaks. Even if structural issues may reduce the actual power surplus, this effect is not negligible: Salvini [9] claims that the ratio between discharge flow rate and GT compressor one must be kept below 15%. This value corresponds to a discharge degree about 0.30, close to the light blue diamond in Fig. 4, allowing for a power surplus of the order of 50% (see Fig. 5). Economic, availability and safety aspects might contribute to further reduction in the useful range of discharge: however, in the

present early stage or the research, we extend the analysis to the whole range of D, in order to include the maximum theoretical performances.

4. WORKING MODES AND SOLUTION STRATEGY

When the load requires less energy than sun can supply, the energy storage device works in charging mode. In principle, the two acting modes of the reciprocating compressor can work either in parallel or series, according to the state of the bottom valve (solid symbol in Fig. 1), respectively fully open or fully closed. The parallel might be useful, to save time and money, during the first charge, when the reservoir has to be filled up to the cushion gas pressure. Preliminary computations demonstrated that, if the tank pressure goes over 500 kPa, no advantage, in terms of charge time and energy saving, is found by working in parallel. Considering that the reservoir pressure must be bigger than turbo-compressor delivery in any time, 500 kPa is selected as the cushion gas value or the minimum pressure, so that the reciprocating compressor acting modes always work in series. Note that the automatic check valves (solid/empty symbol, Fig. 1) assure the proper way to the air flow. Fig. 6 shows the time history of an ideal charge phase: the process starts with the storage at its minimum useful pressure and proceeds until the maximum allowable storage pressure is reached. The positive displacement compressor operates at constant speed. Thus, the increase in storage tank pressure reduces the compressor mass flow (Fig. 6, bottom) and increases the required power (Fig. 5, top). The time integral of compressor power (Fig. 5, middle) shows that a full tank charge cycle requires around 50 kWh, corresponding to half an hour of GT production. During actual operation the charging stops if either we do not have enough power surplus or the reservoir is completely filled.

As above mentioned, unlike the two existing CAES plants, Huntorf (Stys [16]) and McIntosch (Nakhamkin et al. [17]), the discharge mode cannot be decoupled by the gas turbine compressor, so that the storage device must be “idle” or “charging” when the GT is switched off, for instance when solar power fully satisfy the load. It can also be “idle” when GT is working, if stored air is required to be saved for better exploitation.

The control logic and the solution strategy may be summarized as in the following. At each time step we know the difference US between the solar output and the end user load. Furthermore, we decide a priori the time profile of discharge ratio D. At this preliminary stage of the research, three different choices have been considered, namely constant values of D=25%, 50% and 100%, discharging from 6:00 p.m. to 6:00 a.m.. Obviously, the desired discharge may not be actually performed if the tank pressure level is low. The time profile of D could be object of optimization, as future development.

If US is negative, the GT must be switched on. Since both the required power output and *D* are defined, the plant operating point is identified in Fig. 5.

It is worth to note that pollution issues suggest to operate GT above 50% of the design power output. This condition, if we introduce the effect of D, gives us the minimum output power for each curve in Fig. 6. Thus, if US is negative, but its modulus is below this limit, the GT will nonetheless operate at its minimum acceptable output. The surplus power will be used for storage charge, if possible, or wasted.

Fig. 7 provides a sketch of the possible operating conditions. The sun-load gap (i.e., normalized US), in abscissa, defines the GT and storage charge power. Different operating conditions are identified through the color bar at the top of Fig. 7.

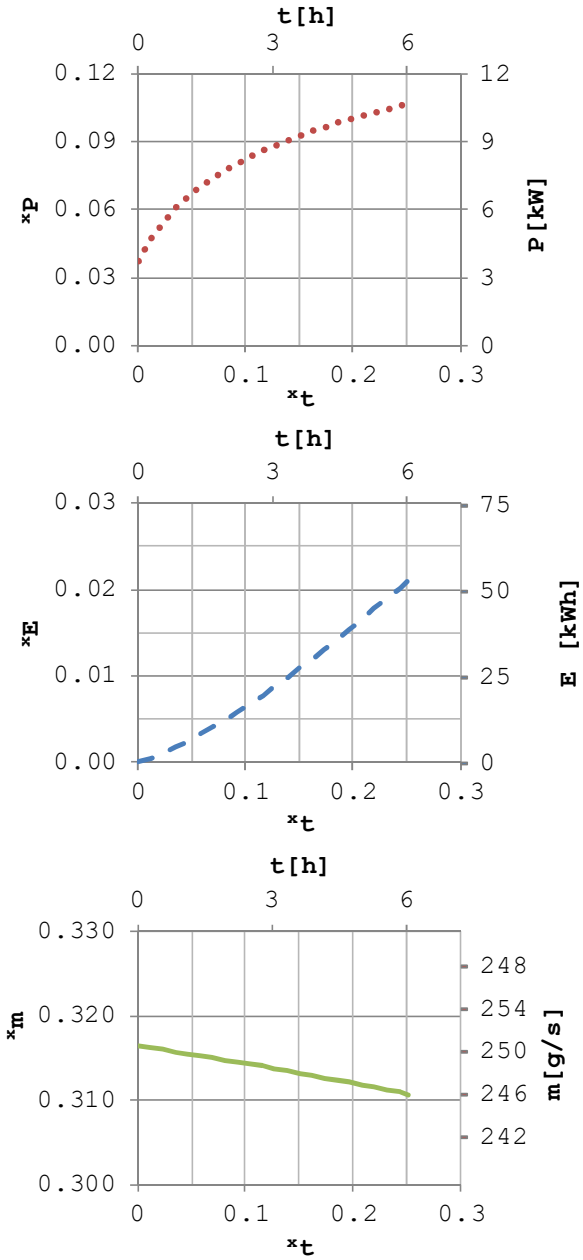

FIGURE 6: CHARGING PHASE TIME HISTORY: FROM TOP TO BOTTOM: RECIPROCATING COMPRESSOR POWER CONSUMPTION, CUMULATIVE ENERGY EXPENDITURE, RECIPROCATING COMPRESSOR MASS FLOW RATE.

In our example the GT power cope with the maximum user load: thus, ${}^{x}P_{US} > -1.0$ under any condition. However, in Fig. 6 we report, in the red zone, also a possible case of higher power demand. We limit the GT power output to 110% of its design value, even in discharge regime, despite the wider range available as in Fig. 6, in order to avoid structural issues and limit the electric equipment cost. The system, thus, cannot satisfy the demand (red zone). When the sun power is not enough to cope with the required load (orange zone), GT must supply this deficit. However, if the required load is less than the minimum operating power suggested by the manufacturer (technical minimum), GT operates at minimum, and the surplus can be utilized by the storage units (yellow zone). Nevertheless, if the storage system is saturated (green zone), the excess must be wasted (or sold, if a grid connection is provided). Of course, some checks are required, for instance, never charging over the structural limit, neither discharging over the cushion gas limit. If we have a solar surplus the GT is off line, and we can charge the reservoir (blue zone). The charging power is limited by the storage compressors size: if this is exceeded (violet zone), part of the solar input will be wasted.

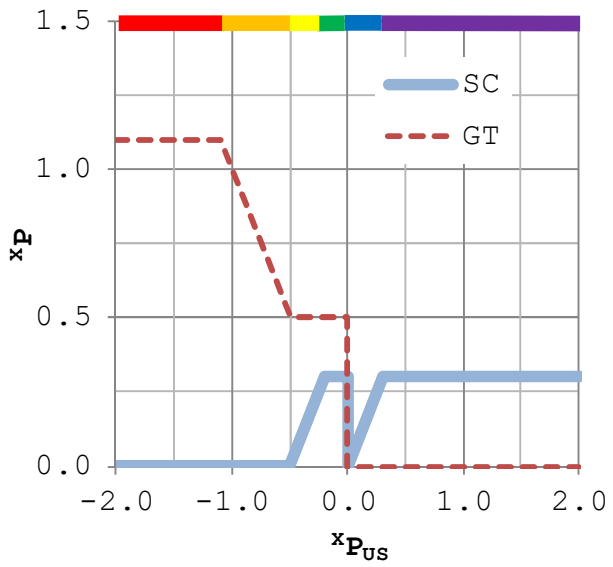

FIGURE 7. GT AND STORAGE COMPRESSOR (SC) POWER VS. SOLAR-USER POWER.

5. TESTS DATA AND RESULTS

In principle, storage systems may be used on a day, week or seasonal time scale. Here, seasonal storage is not feasible, due to the small size, and a weekly one is not interesting: in fact, without a grid connection, it is not possible to exploit the price differences between week-end and working days, which should be the major justification for the cost of a bigger reservoir.

Thus, the analysis will be conducted on a one-day storage period. The tank size is selected to allow a full charge in about six hours, i.e. the time one can think the sun – load surplus US is enough.

The photovoltaic field is sized in order to give exactly the energy required by the electric load, integrated along the same time interval (one day). Thus, with an ideal unit efficiency storage system, no fossil fuel would be necessary. As previously discussed, two different patterns will be analyzed: constant and time-dependent; the latter is scaled from a typical average Italian day [18].

The time profile of the solar energy supply, combined with the variable load, is shown in Fig. 8. The design GT power is enough to cope with the worst scenario of no irradiance, maximum required load and empty storage, thus ensuring supply reliability. As discussed above, we consider three levels of discharge D, namely 0.25, 0.5 and 1.0, and we try to activate the discharge for 12 hours at night time. Results show that at the higher discharge rate D=1 the storage is actually emptied within 3 hours, and at the intermediate D=0.5 in 6 hours.

Since we are considering a single representative day, we need to have periodicity in time. This is achieved numerically running the simulation for a number of days, until the solution stabilizes around a periodic time evolution.

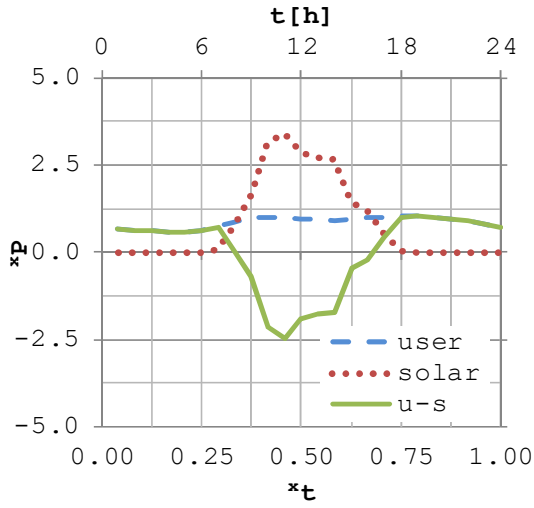

FIGURE 8. SOLAR AND USER TIME SERIES.

As an example, Fig. 9 shows the time series of the cumulative energy exchanges (top and middle) and of discharge and storage parameters D and L (bottom). Results are given for the case "time dependent load, low degree of discharge for long time", which might be the most meaningful. From midnight to 3:00 a.m., with no sun irradiation, GT operates (blue solid line E in top diagram) and makes an optimum use of the storage discharge (air storage energy AS, solid green line, middle diagram), the charge level falls. Then, between 3:00 and 5:00 a.m. the user request is at its minimum, and falls below minimum GT operating condition. Thus, the GT keeps operating at its minimum allowable level, and the power surplus is used to charge the storage. Depending on the conditions, it may happen that charging and discharging operate simultaneously as a kind

power dump. See also the work increase of the storage compressors (blue dashed line SC, middle diagram) and note the first segment at positive slope of the level of storage (dotted red line AS in the lower diagram), which is less steep than the second (7:00-11:00 a.m.), when only discharge is carried out. Then, the storage discharges again, from 7:00 (sunrise), when the sun gives energy both to the user and, up to the air reservoirs filling (11:00 a.m.), the storage compressors. The GT is switched off until 4:00 p.m., when starts again to supply the electrical load, without any storage share. At 6:00 p.m. the storage begins discharge air again, with no further change up to midnight.

Finally, Fig. 10 summarizes the plant performance in terms of both fuel costs saving and storage efficiency, respectively. The former is evaluated, simply, by computing the GT fuel consumption with and without the storage contribution:

$$\Delta Q = Q_{GT,D} - Q_{GT,0} \tag{7}$$

The latter may be defined by the Eq. (8) as the ratio between the energy saved by the GT and the work required by the reciprocating compressors:

$$\eta_{AS} = \frac{E_{GT,D} - E_{GT,0}}{W_{SC}} \tag{8}$$

From an energy point of view, the top figure shows a fuel consumption saving ΔQ for both the constant and the time dependent load, ranging from 7% to 9%, depending on the load and storage managing. In detail, a constant load seems to require a long time, low degree discharge operation, whereas a typical load distribution, with higher demand during sunny hours, the opposite. However, the gap is moderate. The storage efficiency η_{AS} (Fig. 10, middle) does not seem very high, compared with the other storage devices, such as battery, but also hydro pumped storage and even existing CAES (see Arnulfi and Marini [19], [20]).
Finally, it is interesting to remember that the solar field produces, throughout the year, the same energy that is required by the user. Thus, with an ideal lossless storage system we would not have any need for fossil fuel consumption. The actual fuel consumption may be considered a measure of the renewable energy wasted through the process. The bottom picture in Fig. 10 shows the value of Q/E_s for our sample cases. It appears that the renewable energy quota that does not find its way to the user is around 60% in absence of CAES system, and is lowered to 40-50% with the storage system.
Nevertheless, the interest for this kind of device is not to be underestimated, because of its comparatively cheap cost, and its feasibility, since only commercial components are involved. From a sustainability point of view the system avoids the issues related to both the batteries, whose disposal is difficult, and the hydro storage, with well-known critical geological aspect and biosphere interactions.

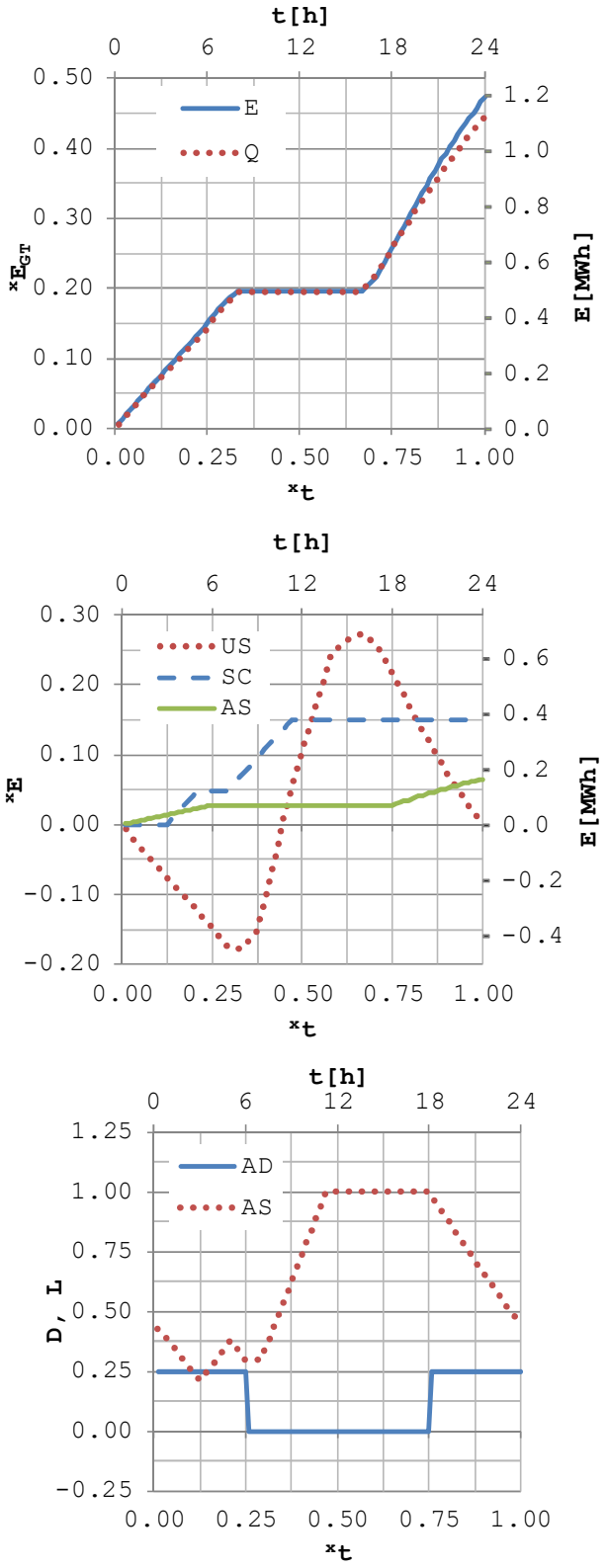

FIGURE 9: PLANT PERFORMANCE, LOW DISCHARGE.

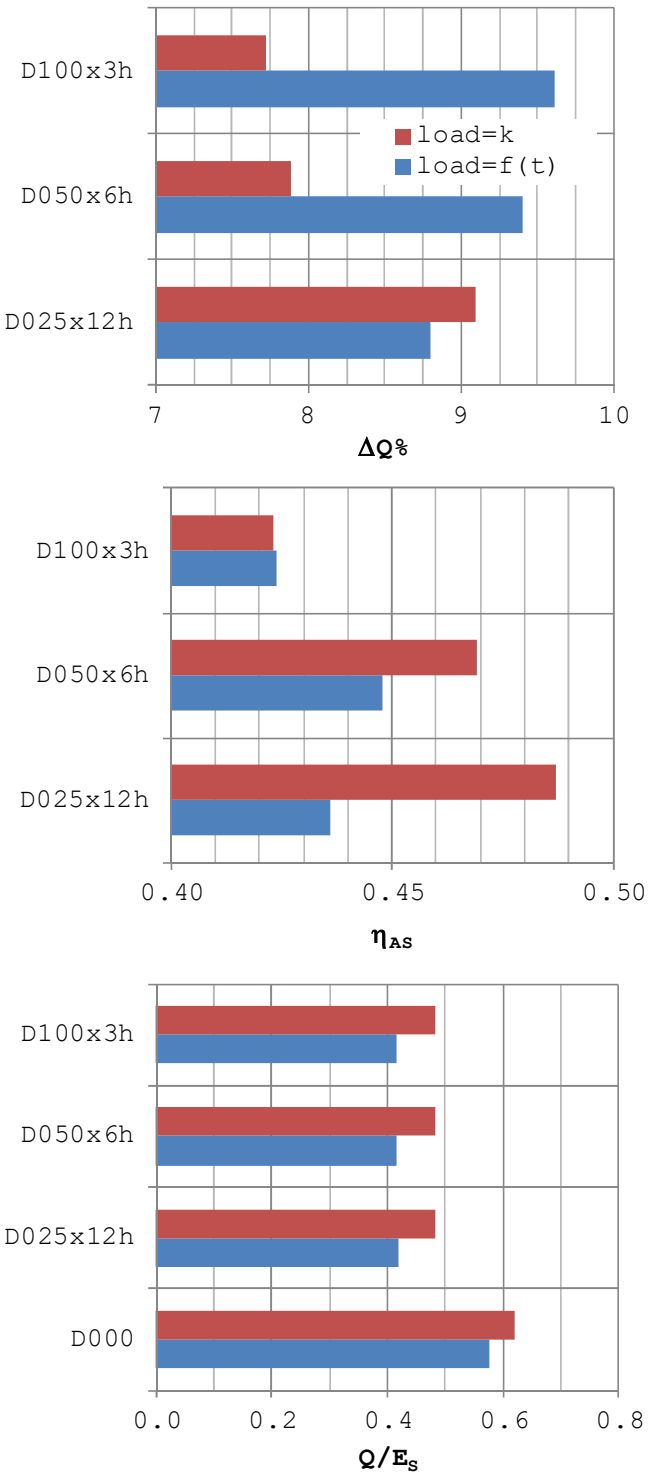

FIGURE 12: GLOBAL PLANT PERFORMANCES

6. CONCLUSIONS AND FUTURE DEVELOPMENT

A stand-alone small power station is analyzed, fed by a photovoltaic system and a micro GT, equipped with a compressed air energy storage device. A lumped parameter model is used, which includes a detailed description and analysis of the GT matching, as well as the operating strategy for the acting modes of the reciprocating compressors.

The CAES storage shows moderate efficiency, lower than most of its possible competitors. However, it still gives significant fuel saving, about 8%. Furthermore, if we consider critical applications, in which a GT or equivalent fossil fuel plant is required to provide safety backup in cloudy days, regardless of the presence of the storage, the fuel saving is obtained with a really modest extra cost, due only to the tank and reciprocating compressors.

The best strategy, in order to maximize the fuel saving, is a function of the load time profile: slow, low mass flow charge is best suited for a user load constant along the day, while a quick, high mass flow charge is preferable for a variable load with higher power demand in daylight hours.

The authors would like to carry on and take into account several boundary conditions, for instance different sun and load patterns, plant configurations, for instance adding grid connection, a battery storage device and a TESTIAC, and finally different approaches, such as a cost analysis, however rough it is, and an optimized sizing procedure.

REFERENCES

[1] Budt, M., Wolf, D., Span, R., Yan, J., 2016, A review on compressed air energy storage: Basic principles, past milestones and recent developments, *Applied Energy*, 170, pp. 250-268.

[2] Kim, Y.-M., Lee, J.-H., Kim, S.-J., Favrat, D., 2012, Potential and evolution of compressed air energy storage: Energy and exergy analyses, *Entropy*, 14 (8), pp. 1501-1521.

[3] Tallini, A., Vallati, A., Cedola, L., 2015, Applications of micro-CAES systems: Energy and economic analysis, *Energy Procedia*, 82, pp. 797-804

[4] Grazzini, G., Milazzo, A., Thermodynamic analysis of CAES/TES systems for renewable energy plants, (2008) *Renewable Energy*, 33 (9), pp. 1998-2006

[5] Tillela, D., Kasinathan, V.V., De Valle, S., Alvarez, M., Frantziskonis, G., Deymier, P., Muralidharan, K., 2010, Compressed-air energy storage systems for stand-alone off-grid photovoltaic modules, IEEE Photovoltaic Specialists Conference, pp. 962-967.

[6] Jannelli, E., Minutillo, M., Lubrano Lavadera, A., Falcucci, G., A small-scale CAES (compressed air energy storage) system for stand-alone renewable energy power plant for a radio base station: A sizing-design methodology, (2014) *Energy*, 78, pp. 313-322.

[7] Zhang, J., Li, K.-J., Wang, M., Lee, W.-J., Gao, H., Zhang, C., Li, K., 2016, A Bi-Level Program for the Planning of an

Islanded Microgrid Including CAES, *IEEE Transactions on Industry Applications*, 52 (4), art. no. 7428931, pp. 2768-2777
[8] Nakhamkin M, Chiruvolu M, Patel M, Byrd S, Schainker R, 2009, "Second Generation of CAES Technology-Performance: Economics, Renewable load Management, Green Energy, POWER-GEN Int., December 8-10, 2009, Las Vegas, NV, USA
[9] Salvini, C., (2015), Techno-economic analysis of small size second generation CAES system, *Energy Procedia*, 82, pp. 782-788
[10] Arnulfi, G.L., Croce, G. and Marini, M., 2007, "Parametric Analysis of Thermal Energy Storage for Gas Turbine Inlet Air Cooling", ASME Paper GT2007-27464.
[11] Rogers, G., and Mayhew, Y, 1992, "Engineerig Thermodynamics, Work and Heat Transfer", Longman, Harlow, United Kingdom.
[12] Cohen, H., Rogers, G. F. C., Saravanamuttoo, H. I. H., 1996, Gas Turbine Theory, Harlow GB, Longman.
[13] Kurzke, J., 1996, "How to Get Components Maps for Aircraft Gas Turbine Performance Calculation", ASME paper 96-GT-164.
[14] Arnulfi, G. L., Cravero, C., and Marini, M., 2012, "Analysis of the Operating Mode Influence onto Energy Consumption of a Natural Gas Storage Plant", ASME paper GT2012-68990.
[15] Pampreen, R.C., 1993, "Compressor Surge and Stall", Concept Eti., Norwitch, VE, USA.
[16] Stys, Z. S., 1980, "Air Storage System Energy Transfer(ASSET) Plants for Peaking", Winter Annual Meeting of ASME, Chicago November 16-21 1980.
[17] Nakhamkin, M., Howard, J., Hoffman, P., Schainker, R. B.,1988,"Reheat 110 MW Turbine with Intercooling for Alabama Electric Cooperative CAES Plant", ASME CogenTurbo, Montreux (Switzerland).
[18] www.mercatoelettrico.org (Italian power, gas and environmental markets operator).
[19] Arnulfi, G. L., and Marini, M., 2006, "Management Strategy for a Compensated Compressed Air Energy Storage Plant", ASME paper GT2006-90437.
[20] Arnulfi, G.L. and Marini, M., 2008, "Performance of a Water Compensated Compressed Air Energy Storage System", ASME Paper GT2008-50627.